Constraining Projected Changes in Rare Intense Precipitation Events Across Global Land Regions

Chao Li[1] , Qiaohong Sun[2], Jianyu Wang[3,4], Yongxiao Liang[5] , Francis W. Zwiers[2,6], Xuebin Zhang[6], and Tong Li[2,6]

[1]Key Laboratory of Geographic Information Science, Ministry of Education | School of Geographic Sciences, East China Normal University, Shanghai, China, [2]Key Laboratory of Meteorological Disaster, Ministry of Education (KLME) | Collaborative Innovation Center on Forecast and Evaluation of Meteorological Disasters (CIC-FEMD), Nanjing University of Information Science & Technology, Nanjing, China, [3]State Key Laboratory of Severe Weather, Chinese Academy of Meteorological Sciences, Beijing, China, [4]University of Chinese Academy of Sciences, Beijing, China, [5]Climate Research Division, Environment and Climate Change Canada, Toronto, ON, Canada, [6]Pacific Climate Impacts Consortium, University of Victoria, Victoria, CO, Canada

Abstract Rare precipitation events with return periods of multiple decades to hundreds of years are particularly damaging to natural and societal systems. Projections of such rare, damaging precipitation events in the future climate are, however, subject to large inter-model variations. We show that a substantial portion of these differences can be ascribed to the projected warming uncertainty, and can be robustly reduced by using the warming observed during recent decades as an observational constraint, implemented either by directly constraining the projections with the observed warming or by conditioning them on constrained warming projections, as verified by extensive model-based cross-validation. The temperature constraint reduces >40% of the warming-induced uncertainty in the projected intensification of future rare daily precipitation events for a climate that is 2°C warmer than preindustrial across most regions. This uncertainty reduction together with validation of the reliability of the projections should permit more confident adaptation planning at regional levels.

Plain Language Summary Very rare extreme precipitation events are particularly damaging to natural and societal systems. Projections of such rare, damaging precipitation events in the future climate vary substantially among climate models. Reducing this uncertainty will aid adaptation planning. We show here that the projected range of future rare precipitation intensification is strongly affected by the projected range of global warming, especially for regions where the intensification is dominated by increases in atmospheric moisture. We verify that using the past global warming trend as an observational constraint can eliminate more than 40% of the warming-induced uncertainty in the intensification of future rare precipitation events at 2°C warmer above preindustrial across most global land regions. This narrowing of the possible range of future rare precipitation intensification at regional scales can greatly benefit adaptation planning.

1. Introduction

Rare precipitation events that occur on average only once during multiple decades are almost always impactful and exceptionally damaging because they occur at the limits of our adaptation to current climate variability, and often expose the extent to which we are not adapted to this variability. With the influence of anthropogenic global warming, precipitation events that would have been rare in the historical context have been occurring increasingly frequent and intense (e.g., Donat et al., 2016; Gillett et al., 2022; Kirchmeier-Young & Zhang, 2020; Min et al., 2011; Paik et al., 2020; Risser & Wehner, 2017; Seneviratne & Zhang, 2021; Sun et al., 2022; Zhang et al., 2013). Each occurrence of such an event motivates questions about future changes to such rare precipitation events that should be considered in the process of adaptation. A prudent, but likely costly approach, would be to plan for the largest plausible changes to rare precipitation events as represented by the upper bound of projections from an ensemble of climate models, which unfortunately present diverging magnitudes of intensification (e.g., Kharin et al., 2013; Li et al., 2021; Wehner et al., 2020). The high cost of adaptation prompts the question of whether the projections of future rare precipitation events can be narrowed and whether the most extreme projections can be discounted. A few observational constraints have been proposed for future moderate precipitation extremes at broad spatial scales (e.g., Borodina et al., 2017; O'Gorman, 2012; Thackeray et al., 2022; Zhang

et al., 2022), with some being verified to have limited utility for rare intense precipitation events (Fergulia et al., 2023). Until now, few studies have reported effective observational constraints on long return period rare precipitation events at regional scales that are more impact-relevant and more informative for adaptation planning.

The thermodynamic property of air characterized by the Clausius-Clapeyron relation indicates that warmer air holds more water vapor, which allows the atmosphere to produce more intense precipitation events (e.g., Allen & Ingram, 2002; Trenberth, 1999). Strong correlations between increases in global mean temperature and the intensity of rare precipitation events at global to regional scales have been noted in both observations and climate model simulations (e.g., Fischer & Knutti, 2016; Fowler et al., 2021; Kharin et al., 2013; Li et al., 2021; Seneviratne & Hauser, 2020; Sun et al., 2021; Westra et al., 2013), suggesting that this link might be useful in constraining projections of future changes in the intensity of rare precipitation events. A range of approaches have been proposed to constrain projections of future warming with constraints of observed warming using, for example, multi-model reweighting (e.g., Liang et al., 2020), detection and attribution-based methods (e.g., Ribes et al., 2021), and the method of emergent constraints (e.g., Chen et al., 2023; Liang et al., 2022; Tokarska et al., 2020).

We show using a computationally intensive cross-validation approach that the observed temperature change over recent decades can also robustly constrain projections of future rare precipitation events at global and regional scales to reduce uncertainty and bias in the projections that is associated with the projected warming. We highlight that the temperature constraint can be implemented equivalently by directly constraining the projections in terms of an emergent constraint method or by conditioning them on constrained warming projections, strengthening confidence in the simple temperature constraint. Given the high cost of adaptation to rare intense precipitation events and the relevant hazards, more precise projections of how much more intense they are likely to become, as reported here, can greatly benefit adaptation efforts at regional scales.

2. Data and Methods

2.1. Projections of Rare Precipitation Events

We focus on daily precipitation events with return periods of 10, 50, and 100 years. An event with return period of T years, also referred to as a T-year event, occurs on average once during a T-year period. We analyze output of 33 climate models in the CMIP6 ensemble (Taylor et al., 2012) and 18 models in the CMIP5 ensemble (Eyring et al., 2016; Table S1 in Supporting Information S1). We consider mainly the 8.5 W/m^2 forcing scenario for future climate projections, that is, the Shared Socioeconomic Pathway 5–8.5 in CMIP6 (O'Neill et al., 2016) and the Representative Concentration Pathway 8.5 in CMIP5 (van Vuuren et al., 2011). We study changes in the intensity of these events in 2028–2057 and 2050–2079, which are 2 and 3°C above the preindustrial 1850–1900 average, respectively, according to the projected global mean surface air temperature (GSAT) changes in these models constrained by the observed GSAT change during 1981–2020 in HadCRUT5 (Morice et al., 2021), as will become evident later. We also provide the results for the mild 4.5 W/m^2 forcing scenario as Supporting Information S1.

We estimate the intensity of a T-year daily precipitation event in a given period by approximating the distribution of the annual maxima of daily precipitation accumulations for that period with a generalized extreme value distribution (GEV; Fischer & Tippett, 1928; Coles, 2001), which has a cumulative distribution function of the form

$$F(x) = \begin{cases} \exp\left[-(1 + \xi(x - \mu)/\sigma)^{-1/\xi}\right], & \xi \neq 0 \\ \exp[-\exp(-(x - \mu)/\sigma)], & \xi = 0 \end{cases}$$

where μ, $\sigma > 0$, and ξ are the location, scale, and shape parameters, respectively. We estimate these parameters by the method of probability weighted moments (Hosking, 1990). The intensity of a T-year event can be calculated by evaluating the inverse of the estimated cumulative distribution function at $1-1/T$.

The intensity of a T-year event is estimated at individual model grid cells by pooling precipitation maxima within a 3×3 grid cell region centered on each grid cell across all available simulations of that model. Doing so reduces

the influence of unforced internal climate variability on the estimated forced intensity changes (e.g., Li et al., 2019; Li et al., 2021), and thus facilitates the determination of physically meaningful emergent constraint relationships for the forced intensity changes. Grid cell estimates of intensity changes in a future period relative to the 1850–1900 baseline are calculated for each climate model. The preindustrial baseline facilitates comparisons of the constrained intensity changes with their unconstrained counterparts assessed in IPCC AR6 (Seneviratne & Zhang, 2021). Estimates of domain median changes over the global land area and in different IPCC AR6 land regions (see Figure S1 in Supporting Information S1 for the geographic boundaries of these regions; Iturbide et al., 2020) are obtained by taking medians of the estimated grid cell changes within the corresponding domains, with one estimate from each climate model. The best estimates of the projected domain median changes and associated uncertainties are inferred from the projected changes by individual models.

2.2. Constraining Precipitation Projections Directly by Emergent Constraint

Among different approaches to framing an emergent constraint function (e.g., Hall et al., 2019; Williamson et al., 2021; Williamson & Sansom, 2019), we adopt the hierarchical emergent constraint method developed in Bowman et al. (2018). Given the observed warming trend as an observational constraint, it represents the constrained projections of changes in the intensity of future rare precipitation events by a Gaussian distribution as follows:

$$Y_{\text{Constrained}} \sim N\left(\hat{\text{M}}_{Y_{\text{Constrained}}}, \hat{\Sigma}^2_{Y_{\text{Constrained}}}\right) \qquad (1)$$

$$\hat{\text{M}}_{Y_{\text{Constrained}}} = \text{M}_{Y_{\text{Raw}}} + \frac{\rho \Sigma_{Y_{\text{Raw}}} \Sigma_{\text{GSAT}}}{\Sigma^2_{\text{GSAT}} + \Sigma_{\text{GSAT\_Obs}}^2} \left(\text{M}_{\text{GSAT\_Obs}} - \text{M}_{\text{GSAT}}\right) \qquad (2)$$

$$\hat{\Sigma}^2_{Y_{\text{Constrained}}} = \Sigma^2_{Y_{\text{Raw}}} \left(1 - \frac{\rho^2}{1 + \Sigma_{\text{GSAT\_Obs}}^2 / \Sigma^2_{\text{GSAT}}}\right) \qquad (3)$$

where $\text{M}_{Y_{\text{Raw}}}$ and $\Sigma_{Y_{\text{Raw}}}$ are the multi-model ensemble mean and standard deviation of the projected changes in the intensity of rare precipitation events in the CMIP6/5 ensemble; M_{GSAT} and Σ_{GSAT} are the ensemble mean and standard deviation of trends in the simulated GSAT over a historical period; ρ is the inter-model correlation coefficient between the projected rare precipitation intensity changes and the simulated historical GSAT trends; $\text{M}_{\text{GSAT\_Obs}}$ and $\Sigma_{\text{GSAT\_Obs}}$ denote the observed GSAT trend and the associated uncertainty placed as the observational constraint. We note that the Gaussian distribution is a reasonable choice for modeling the domain median changes in the intensity of rare precipitation events over the global land and different regions (Figure S2 in Supporting Information S1). As for estimating the projected rare precipitation intensity changes, we employ the multi-member ensemble mean GSAT trend in each climate model so as to reduce the impact of unforced internal variability on a derived emergent relationship. We apply the emergent constraint method to regions only if there exist significant emergent relationships at the 5% level for all considered rare precipitation events (i.e., 10-, 50-, and 100-year events) and projection periods (i.e., 2028–2057 and 2050–2079) under a given future forcing scenario.

We choose the GSAT trend during 1981–2020 as the observable metric considering the fact that GSAT during this period was driven primarily by increasing greenhouse gases and thus can better inform future climate changes forced similarly by greenhouse gases (e.g., Jiménez-de-la-Cuesta & Mauritsen, 2019). We calculate the observed GSAT trend $\text{M}_{\text{GSAT\_Obs}}$ from HadCRUT5 (Morice et al., 2021). The trend in HadCRUT5 reflects changes in blended sea surface temperature over ocean and near-surface air temperature over land and ice with incomplete space-time coverage. In contrast, GSAT trends in climate models represent changes in near-surface air temperature with complete space-time coverage. We therefore scale the HadCRUT5 trend by a factor of 1.074 such that the scaled trend represents the observed globally complete GSAT trend, following from Liang et al. (2020). We use a set of 40-year GSAT time series from preindustrial control simulations of the considered climate models to infer the internal variability in the observed GSAT trend $\Sigma_{\text{GSAT\_Obs}}$ as shown, for example, by the gray shading in Figure 2a.

2.3. Constraining Precipitation Projections Using Constrained Warming

Alternatively, we propose to constrain the projected changes in the intensity of rare precipitation events by conditioning on constrained future warming. We first derive a set of plausible GSAT increases for a future period of interest constrained by the observed 1981–2020 GSAT trend in HadCRUT5, using the same emergent constraint method as described above and illustrated in Figure 2a. Differences among the plausible estimates of GSAT increase reflect uncertainty in the projected warming for a scenario specific future period. Given a plausible estimate of GSAT warming, we identify the first 30-year window with average GSAT exceeding that warming level from each climate model, and estimate changes in the intensity of rare precipitation events in that 30-year window relative to 1850–1900.

We repeat the above procedure for each plausible estimate of GSAT increase, resulting in a collection of estimates of changes in the intensity of rare precipitation events, with an ensemble size of equal to or less than Nx51, where N is the sample size of the constrained plausible GSAT increases generated randomly from the constrained GSAT distribution and 51 is the total number of climate models considered. These estimates of extreme precipitation intensity changes for different 30-year windows are then used to calculate the constrained best estimates and associated uncertainty by assuming a Gaussian distribution inferred from these individual estimates. Here we set $N = 100$ in order to ensure that the inference computation is tractable. Increasing the sample size beyond $N = 100$ does not materially alter the results.

2.4. Model-Based Cross-Validation

It is important to verify that the constrained projections reliably estimate the expected intensification of future rare precipitation events. Future observations are not available, and thus we use simulations from individual climate models as pseudo future observations in an out-of-sample validation approach (Hall et al., 2019; Ribes et al., 2021). Specifically, we evaluate the constrained projections by a model-based cross-validation approach, assuming that good performance across the available ensemble of opportunity (e.g., Tebaldi & Knutti, 2007) will be informative of performance in constraining projections of future observed change. We withhold one model from the CMIP6/5 ensemble of models, treat the projected changes in the intensity of rare precipitation events in the withheld model as "true responses," and use the projected changes in the remaining models to estimate those responses with and without a GSAT constraint from the withheld model. We repeat this procedure for each model and compare the resulting collection of constrained projections with the "true responses."

We assess whether the constrained projections are less biased and how much less uncertain they become compared to unconstrained projections. Bias is defined as the difference between the "true response" and the constrained best estimate, while uncertainty is measured by the width of the constrained central 90% uncertainty range. In addition, we consider the proportion of the constrained 90% uncertainty ranges covering the "true responses." We expect this coverage rate to be consistent with 90%. A substantially smaller coverage rate than the expected value would indicate an overconfident constraint. Although subject to uncertainty due to the use of an ensemble of opportunity (e.g., Tebaldi & Knutti, 2007), model interdependency (e.g., Knutti et al., 2017) and other factors, the cross-validation informs the reliability of using historical temperature change to constrain future rare precipitation intensification.

3. Results

3.1. Uncertain Future Rare Precipitation Intensification

As an example, Figure 1 displays the projected percentage changes in the intensity of 50-year event in a climate that is 2°C warmer than preindustrial (see Table S2 in Supporting Information S1 for the specific values of the event intensity during the preindustrial baseline period). As expected, the 50-year 1-day precipitation event is projected to intensify across global land regions, with high model agreement on the tendency of intensification (>80%) in almost all regions (Figure 1a). Two regional exceptions are found in Caribbean and South-Western South America (hatched in Figure 1a), which are adjacent to subtropical ocean areas with drying precipitation extremes due to changes in atmospheric circulation (e.g., Pfahl et al., 2017). Nevertheless, the climate models project diverging magnitudes of intensification. Over most regions, the width of central 90% range of the projected percentage changes (i.e., the upper bound of the range minus the lower bound; Figure 1b) is more than 30% of the multi-model median change, while the upper bound of the range is about 1.5–2.6 times the multi-model
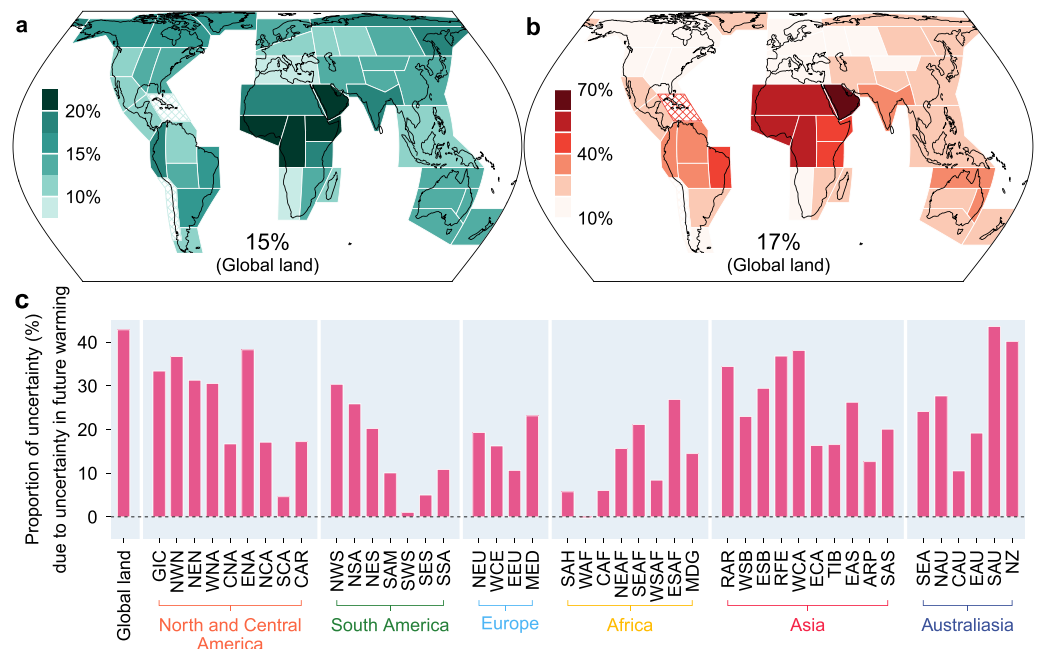
Figure 1. Unconstrained intensification of future 50-year daily precipitation events. (a)–(b) The best estimates (a) and widths of central 90% ranges (b) of changes in the intensity of 50-year daily precipitation event in a climate of 2°C above 1850–1900 (i.e., during 2028–2057 under the 8.5 W/m² scenario) based on unconstrained projections in the CMIP6/5 models. The bottom numbers show values for the global land change. Cross-hatching marks regions where <80% of models project intensification. (c) The proportions of uncertainty in the projected 50-year event intensity changes due to uncertainty in the projected warming in the climate models, quantified by percentage differences between the widths of the central 90% ranges of the intensity changes for the 2028–2057 period and those calculated from individual model 30-year windows reaching the multi-model median warming in global mean surface air temperature projected for 2028–2057. See Figure S1 in Supporting Information S1 for the full names and geographic boundaries of these regions.

median change (not shown). Furthermore, the projected changes diverge even more strongly for the rarer 100-year event and for periods with greater warming (Figure S3 in Supporting Information S1). Such large inter-model spread inevitably hinders adaptation planning and decision making.

It is estimated that about 10%–40% of the inter-model differences in the projected 50-year event intensification over the majority of the regions can be traced to the inter-model differences in the projected warming (Figure 1c), and thus are reducible by constraining uncertainty in the projected warming. The impact of warming uncertainty is large at the global scale because changes in extreme precipitation on average over the global land area are caused mainly by increases in atmospheric moisture, which depends strongly on global warming. Overall, the warming-induced intensification uncertainty is similar to the uncertainty of the intensification contributed from thermodynamic increases in atmospheric moisture in the majority of regions (Figure S4 in Supporting Information S1), suggesting as well the physical basis for a temperature constraint on future rare precipitation intensification.

3.2. Historical Temperature Constraint for Future Rare Precipitation Intensification

Constraining extreme precipitation projections by observed GSAT change requires a robust emergent relationship between the projected changes in future rare precipitation intensity and the historical trends in GSAT during 1981–2020. We find statistically significant such relationships at the 5% level over the global land area and in 31 of the 44 IPCC land regions for the studied rare precipitation events and projection periods. The inter-model correlations between the two quantities range from 0.4 to 0.8 across most regions (Figure S5 in Supporting Information S1).

The regions without a significant emergent relationship generally coincide with areas where changes in atmospheric circulation tend to strongly modulate extreme precipitation (e.g., Gu et al., 2023; O'Gorman & Schneider, 2009; Pfahl et al., 2017). For example, in some subtropical regions such as Central America and the Sahara Desert, dynamic factors such as widening of the Hadley cells can weaken rising motion during rare
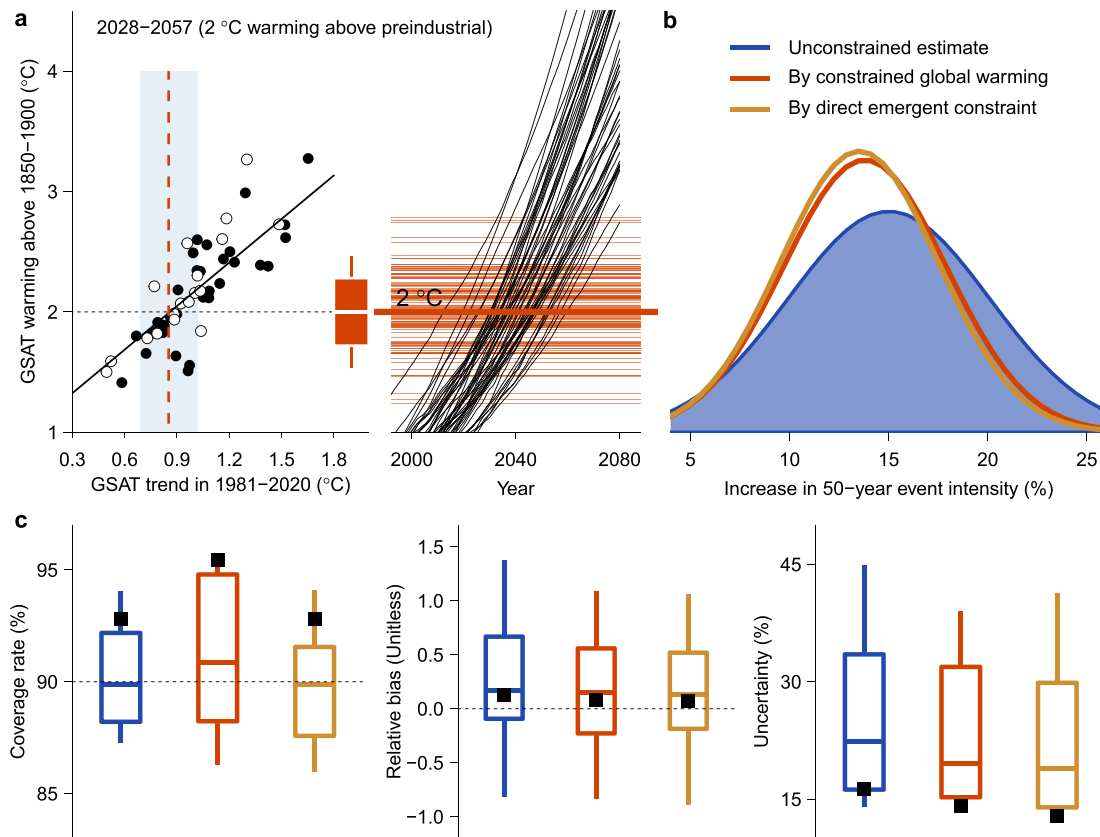
Figure 2. Temperature constraint for the intensification of future rare precipitation events. (a) An illustration of constraining future rare precipitation events based on constrained global warming by the observed 1981–2020 global mean temperature trend with the emergent constraint method (left). The scatter points display global mean temperature changes in 2028–2057 relative to 1850–1900 in response to the 8.5 W/m^2 scenario versus the 1981–2020 global mean temperature trends in CMIP6 (solid points) and CMIP5 (empty points) models. The solid black line shows the emergent constraint regression line. The dashed vertical line and the gray shading mark the observed 1981–2020 global mean temperature trend in HadCRUT5 and associated central 90% uncertainty range due to internal climate variability. Constrained precipitation can be obtained by integrating the projections for 30-year windows reaching the constrained warming levels in the climate models (right; see details in the Data and Methods section). Black curves show 30-year running mean global mean temperatures relative to 1850–1900 in the individual CMIP6/5 models, while horizonal lines depict the constrained plausible 2028–2057 warming levels in response to the 8.5 W/m^2 scenario. (b) The probability density functions of global land change in the intensity of 50-year daily precipitation event in 2028–2057 relative to 1850–1900 under the 8.5 W/m^2 scenario based on unconstrained (blue) and constrained estimates by the observed 1981–2020 global mean temperature trend via constrained global warming (orange) and direct emergent constraint on rare precipitation intensity (brown). (c) Model-based cross-validation of the temperature constraint. Panels show the coverage rates of the central 90% ranges in the estimated intensity changes of rare precipitation events containing the true reference values (left) and the relative biases (middle) and widths of 90% ranges (right) in the estimated changes. Colors of the boxplots distinguish different estimation methods as depicted in (b). The boxplots reflect regional variations, while black rectangles mark values for the global land change. All considered precipitation events during 2028–2057 under the 8.5 W/m^2 scenario are aggregated to compute these validation statistics.

precipitation events (Grise & Davis, 2020; Lu et al., 2007), and thereby offset the effect of atmospheric moistening on precipitation intensification. In contrast, in some semiarid and arid inland regions, such as Central North America and Western Siberia, limited local soil moisture for atmospheric evaporation and the inadequate capacity of atmosphere to transport remote moisture may result in intensification of rare precipitation events weaker than expected from thermodynamics (e.g., Gimeno-Sotelo & Gimeno, 2023). Consequently, the relationship between future rare precipitation intensification and historical GSAT increase is complex in these regions and thus proves ineffective in constraining future rare precipitation intensification (hatched in Figures 3a and 3b).

Apart from such regions, we find that the two constraint approaches produce consistent projections of changes in the intensity of 50-year events for both global land (Figure 2b) and different land regions (Figure S6 in Supporting Information S1), suggesting the robustness of using past warming trend to constrain future rare precipitation intensification. We further gain confidence in the reliability of the constrained projections via a model-based cross-validation analysis. The cross-validation suggests that the temperature constraint implemented in either way can effectively reduce uncertainty and bias in the projections of future rare precipitation intensification (the right two panels in Figure 2c), while the uncertainty of the constrained projections is well

represented by the central 90% uncertainty ranges (the left panel in Figure 2c). For regions without a direct emergent constraint, neither of the two approaches tends to remarkably improve the quality of projections (Figure S7 in Supporting Information S1), highlighting the need for other constraints on atmospheric dynamics for regions where changes in atmospheric circulation strongly modulate the thermodynamic responses of rare precipitation intensity.

The cross-validation also reveals subtle differences between the two constraint approaches. The direct emergent constraint tends to produce projections with slightly smaller bias (middle panel in Figure 2c), presumably because the regional emergent relationships can better accommodate the responses of rare precipitation intensification to thermodynamic processes and feedbacks at regional scales. In contrast, using constrained warming is apt to yield narrower projections (right panel in Figure 2c and Figure S8c in Supporting Information S1), although at the expense of increasing the chance of overconfident projections. For example, for rare precipitation events at a climate of 3°C above the preindustrial (Figure S8c in Supporting Information S1), climate models that do not project strong enough warming up to 2100 will gain less weight (as illustrated by gray curves in Figure S8a in Supporting Information S1).

Overall, the direct emergent constraint exhibits a slightly better tradeoff between bias and uncertainty reduction. Nevertheless, using constrained global warming has additional advantages. First, it enhances confidence in the constrained rare precipitation projections by taking advantage of the warming projections that the IPCC AR6 has assessed to be consistent with different lines of observational evidence in extensive literature (e.g., Lee & Marotzke, 2021; Liang et al., 2020; Ribes et al., 2021; Tokarska et al., 2020). Second, this approach makes it straightforward to link the constrained rare precipitation projections with the policy objectives of the United Nations Framework Convention on Climate Change (IPCC SR15, 2018). Moreover, it allows the investigation of physical processes and compounding hazards associated with constrained rare precipitation events, as it can simultaneously constrain the full fields of different climate variables and thus preserves physical consistency and interactions among different variables. Below, we combine the two approaches to map the projected intensification of rare precipitation events across global land regions, using the constrained warming method for regions without a direct emergent constraint relationship.

3.3. Constrained Future Rare Precipitation Intensification

Figures 3a and 3b show the counterparts of Figures 1a and 1b constrained by the observed GSAT trend during 1981–2020 from HadCRUT5 (see Table S2 in Supporting Information S1 for specific values of the constrained changes). Almost everywhere, the constrained projections show less intensification of future 50-year daily precipitation events than unconstrained projections (Figure 3a vs. Figure 1a) and remarkably narrower 90% uncertainty ranges (Figure 3b vs. Figure 1b). For the 50-year event intensity in a climate that is 2°C above preindustrial in most regions, the best estimates of the projected change are calibrated downward by 8%–18% relative to unconstrained projections (Figure 3c), while the constrained central 90% ranges are 10%–30% narrower than the unconstrained values (Figure 3d). In more than half of the regions, the reduced uncertainty amounts to over 40% of the intensification uncertainty induced by the projected warming uncertainty (i.e., ratios of values in Figures 3d and 1c). Moreover, the upper bounds of the central 90% ranges, which would dominate the cost of prudent regional adaptation and climate resilience policy that minimize future risk, are reduced by more than 8%–15% for most regions (Figure 3e), reflecting a reduction in the influence of high-sensitivity climate models in the constrained projections.

On average over the global land, the constrained intensification of 50-year event is projected to be 13.5% (7%–20.1% for central 90% range) for a climate that is 2°C warmer than preindustrial (i.e., by 2028–2057 under the 8.5 W/m^2 forcing scenario; brown curve in Figure 2b). This is in line with the expectation from atmospheric moisture increase as predicted by the Clausius-Clapeyron relation. This consistency also suggests the robustness of the temperature constraint on the intensification of future rare precipitation dominated by thermodynamics. At regional scales, the most pronounced uncertainty reduction occurs to Northern Hemisphere middle to high latitudes and Asian monsoon regions (Figures 3b and 3d). These regions show relatively stronger relationships between the projected rare precipitation intensification and the 1981–2020 GSAT warming (Figure S5 in Supporting Information S1), resulting from the dominating thermodynamic contributions to the overall responses of rare precipitation intensity in these regions (Figure S4 in Supporting Information S1; e.g., Pfahl et al., 2017). Despite the considerable uncertainty reduction in the tropical and subtropical regions, the relative uncertainty of
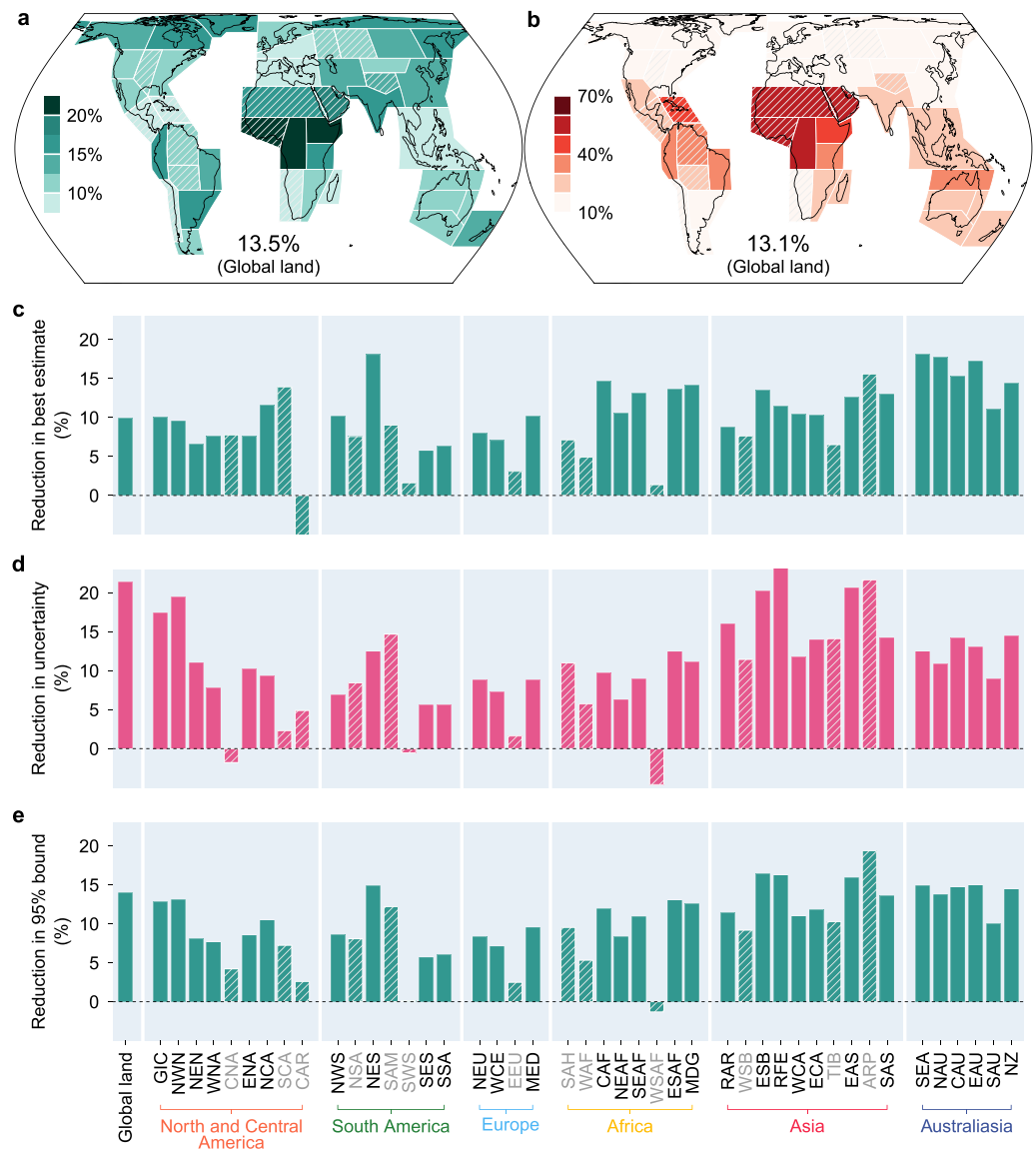
Figure 3. Intensification of future 50-year daily precipitation events constrained by the past observed warming trend. (a)–(b) The best estimates (a) and widths of the central 90% ranges (b) of changes in the intensity of 50-year daily precipitation event in a climate of 2°C above 1850–1900 (i.e., during 2028–2057 under the 8.5 W/m^2 scenario) constrained by the observed 1981–2020 global mean temperature trend. The bottom numbers show values for the global land change. (c)–(d) The percentage reductions in the constrained best estimates (c) and widths (d) and upper bounds (e) of the central 90% ranges relative to the corresponding values in unconstrained projections. Direct emergent constraint on precipitation is adopted for regions with significant emergent relationships at the 5% level for all considered rare precipitation events and projection periods (solid shading). Constrained future warming are used to constrain precipitation in other regions (hatched shading). See Figure S1 in Supporting Information S1 for the full names and geographic boundaries of these regions.

the constrained projections remains largest in these regions (Figure 3b). Improving the simulation of relevant processes such as moist convection in the tropics and identifying observational constraints on changes in relevant atmospheric circulations in the subtropics should be explored as a matter of urgency.

We note that the relative uncertainty reduction does not vary strongly among rare precipitation events or future periods (Figure S9 in Supporting Information S1 vs. Figures 3c–3e). Interestingly, the temperature constraint tends to produce more pronounced uncertainty reduction if the intensification of future rare precipitation events is evaluated against a more recent reference period (e.g., 1950–2000; Figure S10 in Supporting Information S1) and/or under a relatively milder forcing scenario (e.g., the 4.5 W/m^2 scenario; Figures S11 and S12 in Supporting

Information S1). This is partly because of the relatively narrower inter-model spread of the unconstrained projections confined by the relatively weaker warming in such situations, which facilitate stronger emergent constraint relationships (top panels in Figures S10–S12 in Supporting Information S1) and thus more relative uncertainty reductions (as evidenced from Equation 3; pink bars in Figures S10–S12 in Supporting Information S1). Figures S13 and S14 in Supporting Information S1 visualize the impact of the choice of reference period and future forcing scenario on the emergent constraint relationships for some selected regions. Finally, we emphasize that the results reported here are robust to the use of other observational temperature data sets thanks to the consistent GSAT trends during recent decades in different data sets (e.g., Gulev et al., 2021; Shiogama et al., 2022; Tokarska et al., 2020).

Another relevant question is whether the observed past warming trend is also able to effectively constrain projections of changes in the frequency of future rare precipitation events. In fact, the response of rare precipitation frequency to global warming is strongly nonlinear (e.g., Kharin et al., 2018; Li et al., 2021). As a result, the projected changes in the frequency of future rare precipitation events in most regions correlate weakly with historical GSAT trends (Figure S15 in Supporting Information S1). Thus, the observed past warming trend cannot serve as an effective *linear* constraint on the frequency of future rare precipitation events, in line with a recent study on constraining the global increase of extreme precipitation frequency using its historical trend rather than the past global warming trend (Thackeray et al., 2022).

4. Conclusions

We show that the observed global warming trend over the recent past decades provides a robust and efficient constraint for the intensification of future rare, damaging precipitation events, particularly when the intensification is dominated by changes in thermodynamic processes. For changes in the intensity of daily precipitation events with return periods of 10–100 years in a future period that is 2°C above preindustrial, the constraint narrows the projected central 90% uncertainty range by 10%–30% across most regions, while substantially lowering the upper bound of the uncertainty range that is relevant for prudent adaptation efforts. The reduced uncertainty amounts to over 40% of the inter-model variations induced by the projected warming uncertainty. The constraint also reduces the projected intensification of these rare precipitation events by 8%–18% weaker compared to unconstrained projections.

Nevertheless, the past warming trend is less effective in constraining the intensification of future rare precipitation events in some tropical and subtropical regions where changes in atmospheric circulation play a substantial role in the intensification while model consensus on the underlying dynamic mechanisms is low (e.g., O'Gorman, 2012; O'Gorman & Schneider, 2009). Identifying observational constraints on changes in relevant atmospheric circulations in such regions should be explored in future as a matter of urgency. In addition, the spatial patterns of sea surface temperature warming (e.g., Chadwick, 2016; Zhang et al., 2023) and low-level cloud properties (e.g., Liang et al., 2022; Zhou et al., 2023) have been identified as influencing factors for both warming and seasonal mean precipitation change at regional to global scales and should be further explored for rare precipitation extremes.

Overall, the simple temperature constraint can be understood as preferentially weighting models with transient climate responses that are consistent with the observed warming over the recent past decades. More accurate projections of rare, damaging precipitation events can be expected as the ability of contemporary climate models to simulate rare precipitation events continues to improve and the uncertainty in transient climate response is further reduced. We believe that the reported narrowing of uncertainty in the projected intensification of future rare, damaging precipitation events at regional levels together with our validation of the reliability of the projections should permit more confident regional adaptation planning.

Data Availability Statement

All the data sets analyzed in this study are publicly available. The HadCRUT5 temperature observations are available at Morice et al. (2021). The CMIP6 climate model simulations are available at Eyring et al. (2016), while the CMIP5 simulations are available at Taylor et al. (2012). The CMIP6 and CMIP5 models used in this study can be found in Table S1 of the Supporting Information S1.

References

Allen, M. R., & Ingram, W. J. (2002). Constraints on future changes in climate and the hydrological cycle. *Nature*, *419*(6903), 224–232. https://doi.org/10.1038/nature01092

Borodina, A., Fischer, E. M., & Knutti, R. (2017). Models are likely to underestimate increase in heavy rainfall in the extratropical regions with high rainfall intensity. *Geophysical Research Letters*, *44*(14), 7401–7409. https://doi.org/10.1002/2017gl074530

Bowman, K. W., Cressie, N., Qu, X., & Hall, A. (2018). A hierarchical statistical framework for emergent constraints: Application to snow-albedo feedback. *Geophysical Research Letters*, *45*(23), 13050–13059. https://doi.org/10.1029/2018gl080082

Chadwick, R. (2016). Which aspects of CO_2 forcing and SST warming cause most uncertainty in projections of tropical rainfall change over land and ocean? *Journal of Climate*, *29*(7), 2493–2509. https://doi.org/10.1175/jcli-d-15-0777.1

Chen, Z., Zhou, T., Chen, X., Zhang, W., Zuo, M., Man, W., & Qian, Y. (2023). Emergent constrained projections of mean and extreme warming in China. *Geophysical Research Letters*, *50*(20), e2022GL102214. https://doi.org/10.1029/2022gl102124

Coles, S. G. (2001). *An introduction to statistical modeling of extreme values*. Springer.

Donat, M. G., Lowry, A. L., Alexander, L. V., O'Gorman, P. A., & Maher, N. (2016). More extreme precipitation in the world's dry and wet regions. *Nature Climate Change*, *6*(5), 508–513. https://doi.org/10.1038/nclimate2941

Eyring, V., Bony, S., Meehl, G. A., Senior, C. A., Stevens, B., Stouffer, R. J., et al. (2016). The coupled model intercomparison project phase 6 (CMIP6) [Dataset]. Retrieved from https://wcrp-cmip.org/cmip-data-access/

Fergulia, O., von Hardenberg, J., & Palazzi, E. (2023). Robustness of precipitation emergent constraints in CMIP6 models. *Climate Dynamics*, *61*(3–4), 1439–1450. https://doi.org/10.1007/s00382-022-06634-1

Fischer, E. M., & Knutti, R. (2016). Observed heavy precipitation increase confirms theory and early models. *Nature Climate Change*, *6*(11), 986–991. https://doi.org/10.1038/nclimate3110

Fischer, E. M., & Tippett, H. C. (1928). Limiting forms of the frequency distribution of the largest or smallest members of a sample. *Proceedings of the Cambridge Philosophical Society*, *24*, 180–190.

Fowler, H. J., Lenderink, G., Prein, A. F., Westra, S., Allan, R. P., Ban, N., et al. (2021). Anthropogenic intensification of short-duration rainfall extremes. *Nature Reviews Earth & Environment*, *2*, 107–122. https://doi.org/10.1038/s43017-020-00128-6

Gillett, N. P., Cannon, A. J., Malinina, E., Schnorbus, M., Anslow, F., Sun, Q., et al. (2022). Human influence on the 2021 British Columbia floods. *Weather and Climate Extremes*, *36*, 100441. https://doi.org/10.1016/j.wace.2022.100441

Gimeno-Sotelo, L., & Gimeno, L. (2023). Where does the link between atmospheric moisture transport and extreme precipitation matter? *Weather and Climate Extremes*, *39*, 100536. https://doi.org/10.1016/j.wace.2022.100536

Grise, K. M., & Davis, S. M. (2020). Hadley cell expansion in CMIP6 models. *Atmospheric Chemistry and Physics*, *20*(9), 5249–5268. https://doi.org/10.5194/acp-20-5249-2020

Gu, L., Yin, J., Gentine, P., Awang, H., Slater, L. J., Sullivan, S. C., et al. (2023). Large anomalies in future extreme precipitation sensitivity driven by atmospheric dynamics. *Nature Communications*, *14*(1), 3197. https://doi.org/10.1038/s41467-023-39039-7

Gulev, S. K., Thorne, P. W., Ahn, J., Dentener, F. J., Domingues, C. M., Gerland, S., et al. (2021). Changing State of the Climate System. In *Climate change 2021: The physical science basis. Contribution of Working Group I to the Sixth Assessment Report of the Intergovernmental Panel on Climate Change* [Masson-Delmotte, V., Zhai, P., Pirani, A., Connoers, S. L., Péan, C., Berger, S., et al. (eds.)]. Cambridge University Press, Cambridge, United Kingdom and New York, NY, USA, pp. 287-422. https://doi.org/10.1017/9781009157896.004

Hall, A., Cox, P., Huntingford, C., & Klein, S. (2019). Progressing emergent constraints on future climate change. *Nature Climate Change*, *9*(4), 269–278. https://doi.org/10.1038/s41558-019-0436-6

Hosking, J. R. M. (1990). L-moments: Analysis and estimation of distributions using linear combination of order statistics. *Journal of the Royal Statistical Society*, *52B*, 105–124.

IPCC. (2018). *Global warming of 1.5°C. An IPCC Special Report on the impacts of global warming of 1.5°C above pre-industrial levels and related global greenhouse gas emission pathways, in the context of strengthening the global response to the threat of climate change, sustainable development, and efforts to eradicate poverty* [Masson-Delmotte, V., Zhai, P., Pörtner, H.-O., Roberts, D., Skea, J., Shukla, P. R., et al. (eds.)]. Cambridge University Press, Cambridge, UK and New York, NY, USA, 616 pp. https://doi.org/10.1017/9781009157940

Iturbide, M., Gutiérrez, J. M., Alves, L. M., Bedia, J., Cerezo-Mota, R., Cimadevilla, E., et al. (2020). An update of IPCC climate reference regions for subcontinental analysis of climate model data: Definition and aggregated datasets. *Earth System Science Data*, *12*(4), 2959–2970. https://doi.org/10.5194/essd-12-2959-2020

Jiménez-de-la-Cuesta, D., & Mauritsen, T. (2019). Emergent constraints on Earth's transient and equilibrium response to doubled CO2 from post-1970s global warming. *Nature Geoscience*, *12*(11), 902–905. https://doi.org/10.1038/s41561-019-0463-y

Kharin, V. V., Flato, G. M., Zhang, X., Gillett, N. P., Zwiers, F. W., & Anderson, K. J. (2018). Risks from climate extremes change differently from 1.5°C to 2.0°C depending on rarity. *Earth's Future*, *6*(5), 704–715. https://doi.org/10.1002/2018ef000813

Kharin, V. V., Zwiers, F. W., Zhang, X., & Wehner, M. (2013). Changes in temperature and precipitation extremes in the CMIP5 ensemble. *Climate Change*, *119*(2), 345–357. https://doi.org/10.1007/s10584-013-0705-8

Kirchmeier-Young, M. C., & Zhang, X. (2020). Human influence has intensified extreme precipitation in North America. *Proceedings of the National Academy of Sciences of the United States of America*, *117*(24), 13308–13313. https://doi.org/10.1073/pnas.1921628117

Knutti, R., Sedláček, J., Sanderson, B. M., Lorenz, R., Fischer, E. M., & Eyring, V. (2017). A climate model projection weighting scheme accounting for performance and interdependence. *Geophysical Research Letters*, *44*(4), 1909–1918. https://doi.org/10.1002/2016gl072012

Lee, J.-Y., Marotzke, J., Bala, G., Cao, L., Corti, S., Dunne, J. P., et al. (2021). Future Global Climate: Scenario-based Projections and Near-Term Information. In *Climate change 2021: The physical science basis. Contribution of Working Group I to the Sixth Assessment Report of the Intergovernmental Panel on Climate Change* [Masson-Delmotte, V., Zhai, P., Pirani, A., Connoers, S. L., Péan, C., Berger, S., et al. (eds.)]. Cambridge University Press, Cambridge, United Kingdom and New York, NY, USA, pp. 553-672. https://doi.org/10.1017/9781009157896.006

Li, C., Zwiers, F. W., Zhang, X., & Li, G. (2019). How much information is required to well constrain local estimates of future precipitation extremes? *Earth's Future*, *7*(1), 11–24. https://doi.org/10.1029/2018ef001001

Li, C., Zwiers, F. W., Zhang, X., Li, G., Sun, Y., & Wehner, M. (2021). Changes in annual extremes of daily temperature and precipitation in CMIP6 models. *Journal of Climate*, *34*(9), 3441–3460. https://doi.org/10.1175/jcli-d-19-1013.1

Liang, Y., Gillett, N. P., & Monahan, A. H. (2020). Climate model projections of 21st century global warming constrained using the observed warming trend. *Geophysical Research Letters*, *47*(12), e2019GL086757. https://doi.org/10.1029/2019gl086757

Liang, Y., Gillett, N. P., & Monahan, A. H. (2022). Emergent constraints on CMIP6 climate warming projections: Contrasting cloud- and surface-temperature-based constraints. *Journal of Climate*, *35*(6), 1809–1824. https://doi.org/10.1175/jcli-d-21-0468.1

Lu, J., Vecchi, G. A., & Reichler, T. (2007). Expansion of the Hadley cell under global warming. *Geophysical Research Letters*, *34*(6), L06805. https://doi.org/10.1029/2006gl028443

Min, S. K., Zhang, X., Zwiers, F. W., & Hegerl, G. C. (2011). Human contribution to more-intense precipitation extremes. *Nature*, *470*(7334), 378–381. https://doi.org/10.1038/nature09763

Morice, C. P., Kennedy, J. J., Rayner, N. A., Winn, J. P., Hogan, E., Killick, R. E., et al. (2021). An updated assessment of near-surface temperature change from 1850: The HadCRUT5 data set [Dataset]. Journal of Geophysical Research: Atmospheres, *126*(3), e2019JD032361. https://doi.org/10.1029/2019jd032361

O'Gorman, P. A. (2012). Sensitivity of tropical precipitation extremes to climate change. *Nature Geoscience*, *5*(10), 697–700. https://doi.org/10.1038/ngeo1568

O'Gorman, P. A., & Schneider, T. (2009). The physical basis for increases in precipitation extremes in simulations of 21st-century climate change. *Proceedings of the National Academy of Sciences*, *106*(35), 14773–14777. https://doi.org/10.1073/pnas.0907610106

O'Neill, B. C., Tebaldi, C., van Vuuren, D. P., Eyring, V., Friedlingstein, P., Hurtt, G., et al. (2016). The scenario model intercomparison project (ScenarioMIP) for CMIP6. *Geoscientific Model Development*, *9*, 3461–3482. https://doi.org/10.5194/gmd-9-3461-2016

Paik, S., Min, S., Zhang, X., Donat, M. G., King, A. D., & Sun, Q. (2020). Determining the anthropogenic greenhouse gas contribution to the observed intensification of extreme precipitation. *Geophysical Research Letters*, *47*(12), e2018GL086875. https://doi.org/10.1029/2019gl086875

Pfahl, S., O'Gorman, P. A., & Fischer, E. M. (2017). Understanding the regional pattern of projected future changes in extreme precipitation. *Nature Climate Change*, *7*(6), 423–427. https://doi.org/10.1038/nclimate3287

Ribes, A., Qasmi, S., & Gillett, N. P. (2021). Making climate projections conditional on historical observations. *Science Advances*, *7*(4), eabc0671. https://doi.org/10.1126/sciadv.abc0671

Risser, M. D., & Wehner, M. F. (2017). Attributable human-induced changes in the likelihood and magnitude of the observed extreme precipitation during hurricane Harvey. *Geophysical Research Letters*, *44*(24), 12457–12464. https://doi.org/10.1002/2017gl075888

Seneviratne, S. I., & Hauser, M. (2020). Regional climate sensitivity of climate extremes in CMIP6 versus CMIP5 multimodel ensembles. *Earth's Future*, *8*(9), e2018EF001474. https://doi.org/10.1029/2019ef001474

Seneviratne, S. I., Zhang, X., Adnan, M., Badi, M., Dereczynski, C., Di Luca, A., et al. (2021). Weather and Climate Extremes in a Changing Climate. In *Climate change 2021: The physical science basis. Contribution of Working group I to the Sixth Assessment Report of the Intergovernmental Panel on Climate Change* [Masson-Delmotte, V., Zhai, P., Pirani, A., Connoers, S. L., Péan, C., Berger, S., et al. (eds.)]. Cambridge University Press, Cambridge, United Kingdom and New York, NY, USA, pp. 1513-1766. https://doi.org/10.1017/9781009157896.013

Shiogama, H., Watanabe, M., Kim, H., & Hirota, N. (2022). Emergent constraints on future precipitation changes. *Nature*, *602*(7898), 612–616. https://doi.org/10.1038/s41586-021-04310-8

Sun, Q., Zhang, X., Zwiers, F. W., Westra, S., & Alexander, L. V. (2021). A global, continental, and regional analysis of changes in extreme precipitation. *Journal of Climate*, *34*(1), 243–258. https://doi.org/10.1175/jcli-d-19-0892.1

Sun, Q., Zwiers, F. W., Zhang, X., & Yan, J. (2022). Quantifying the human influence on the intensity of extreme 1- and 5-day precipitation amounts at global, continental, and regional scales. *Journal of Climate*, *35*, 195–210.

Taylor, K. E., Stouffer, R. J., & Meehl, G. A. (2012). The coupled model intercomparison project phase 5 (CMIP5) [Dataset]. Retrieved from https://wcrp-cmip.org/cmip-phase-5-cmip5/

Tebaldi, C., & Knutti, R. (2007). The use of multi-model ensemble in probabilistic climate projections. *Philosophical Transactions of the Royal Society*, *365*(1857), 2053–2075. https://doi.org/10.1098/rsta.2007.2076

Thackeray, C. W., Hall, A., Norris, J., & Chen, D. (2022). Constraining the increased frequency of global precipitation extremes under warming. *Nature Climate Change*, *12*(5), 441–448. https://doi.org/10.1038/s41558-022-01329-1

Tokarska, K. B., Stolpe, M. B., Sippel, S., Fischer, E. M., Smith, C. J., Lehner, F., & Knutti, R. (2020). Past warming trend constrains future warming in CMIP6 models. *Science Advances*, *6*(12), eaaz9549. https://doi.org/10.1126/sciadv.aaz9549

Trenberth, K. E. (1999). Conceptual framework for changes of extremes of the hydrological cycle with climate change. *Climate Change*, *42*(1), 327–339. https://doi.org/10.1023/a:1005488920935

van Vuuren, D. P., Edmonds, J., Kainuma, M., Riahi, K., Thomson, A., Hibbard, K., et al. (2011). The representative concentration pathways: An overview. *Climate Change*, *109*(1–2), 5–31. https://doi.org/10.1007/s10584-011-0148-z

Wehner, M., Gleckler, P., & Lee, J. (2020). Characterization of long period return values of extreme daily temperature and precipitation in the CMIP6 models: Part 1, model evaluation. *Weather and Climate Extremes*, *30*, 100283. https://doi.org/10.1016/j.wace.2020.100283

Westra, S., Alexander, L. V., & Zwiers, F. W. (2013). Global increasing trends in annual maximum daily precipitation. *Journal of Climate*, *26*(11), 3904–3918. https://doi.org/10.1175/jcli-d-12-00502.1

Williamson, D. B., & Sansom, P. G. (2019). How are emergent constraints quantifying uncertainty and what do they leave behind? *Bulletin of the American Meteorological Society*, *100*(12), 2571–2588. https://doi.org/10.1175/bams-d-19-0131.1

Williamson, M. S., Trackeray, C. W., Peter, M. C., Hall, A., Huntingford, C., & Nijsse, J. M. M. (2021). Emergent constraints on climate sensitivities. *Reviews of Modern Physics*, *93*(2), 025004. https://doi.org/10.1103/revmodphys.93.025004

Zhang, S., Stier, P., Dagan, G., Zhou, C., & Wang, M. (2023). Sea surface warming patterns drive hydrological sensitivity uncertainties. *Nature Climate Change*, *13*(6), 545–553. https://doi.org/10.1038/s41558-023-01678-5

Zhang, W., Furtado, K., Zhou, T., Wu, P., & Chen, X. (2022). Constraining extreme precipitation projections using past precipitation variability. *Nature Communications*, *13*(1), 6319. https://doi.org/10.1038/s41467-022-34006-0

Zhang, X., Wan, H., Zwiers, F. W., Hegerl, G. C., & Min, S. K. (2013). Attributing intensification of precipitation extremes to human influence. *Geophysical Research Letters*, *40*(19), 5252–5257. https://doi.org/10.1002/grl.51010

Zhou, W., Leung, L. R., Siler, N., & Lu, J. (2023). Future precipitation increase constrained by climatological pattern of cloud effect. *Nature Communications*, *14*(1), 6363. https://doi.org/10.1038/s41467-023-42181-x